Mathematical Models of Tumour and Normal Tissue Response

Bleddyn Jones and Roger G. Dale

From the Clatterbridge Centre for Oncology, Liverpool/Wirral (B. Jones), and the Department of Radiation Physics & Radiobiology, Charing Cross Hospital, London (R.G. Dale), UK

Correspondence to: Dr Bleddyn Jones, Reader in Oncology, Imperial College of Medicine, Hammersmith Hospital, Du Cane Road, London W12 0HS, UK

Acta Oncologica Vol. 38, No. 7, pp. 883–893, 1999

The historical application of mathematics in the natural sciences and in radiotherapy is compared. The various forms of mathematical models and their limitations are discussed. The Linear Quadratic (LQ) model can be modified to include (i) radiobiological parameter changes that occur during fractionated radiotherapy, (ii) situations such as focal forms of radiotherapy, (iii) normal tissue responses, and (iv) to allow for the process of optimization. The inclusion of a variable cell loss factor in the LQ model repopulation term produces a more flexible clonogenic doubling time, which can simulate the phenomenon of 'accelerated repopulation'. Differential calculus can be applied to the LQ model after elimination of the fraction number integers. The optimum dose per fraction (maximum cell kill relative to a given normal tissue fractionation sensitivity) is then estimated from the clonogen doubling times and the radiosensitivity parameters (or α/β ratios). Economic treatment optimization is described. Tumour volume studies during or following teletherapy are used to optimize brachytherapy. The radiation responses of both individual tumours and tumour populations (by random sampling 'Monte-Carlo' techniques from statistical ranges of radiobiological and physical parameters) can be estimated. Computerized preclinical trials can be used to guide choice of dose fractionation scheduling in clinical trials. The potential impact of gene and other biological therapies on the results of radical radiotherapy are testable. New and experimentally testable hypotheses are generated from limited clinical data by exploratory modelling exercises.

Received 12 August 1998
Accepted 8 March 1999

The main requirement for a satisfactory mathematical model of any process is that the equation(s) must provide a reasonably accurate assessment of the fluctuations in outcome following changes in the initial conditions. In general, mathematical modelling techniques answer the question, 'what if', when applied to numerical problems. Unlike the case with physics, engineering and biology, the application of such models in medicine has been limited. Medical decisions usually require a combination of knowledge and experience in order to analyse and interpret symptoms, physical signs, images and biochemical parameters. This form of decision-making is unsuitable in complex non-linear processes, to an extent that computational methods are indicated.

HISTORY OF MODELLING IN THE NATURAL SCIENCES

Historical modelling examples include the classical deterministic relationships between velocity, distance and time enunciated by Galileo and Newton. Nowadays, deterministic models are routinely used in the computerized design of cars, aircraft, industrial production, and so on. Much of Newtonian mechanics involves a balancing of opposing forces for which optimized solutions may be found, using calculus. There are interesting parallels to this in the optimization of radiotherapy, where total tumour dose must be balanced against normal tissue toxicity and overall treatment time is balanced against tumour cell repopulation.

All models have limitations, as Einstein demonstrated of the Newtonian model of the Universe. Similarly, Schroedinger's work showed that deterministic models cannot adequately describe the behaviour of subatomic particles. Although quantum mechanics and relativity are not yet fully compatible within any unified theory, in their particular domains each model is highly accurate. Perhaps this is the extreme example of models being useful even when the entire process is not fully understood.

Similar examples are found in the field of biology. Deterministic models, for example the population growth models of Fibonacci, Malthus (1) and the later developments by authorities such as D'Arcy Thompson (2) and J Maynard Smith (3), have resulted in many practical applications. Further progress resulted from statistical distribu-

 ISSN 0284-186X

tion models such as the 't' and 'χ^2', which are routinely used to determine the statistical significance of experimental outcomes in the presence of random biological variation.

The mechanism of radiation action relies upon the production of random lesions within the genome. Relatively low radiation doses cause rare sporadic effects such as leukaemogenesis (4). At higher doses, such as those used in radiotherapy, the accumulation of many random lesions produces a more predictable (and deterministic) outcome, which translates to radiation dose–response curves for tumour control and normal tissue effects. Although likely to be complex, modelling of radiation-induced gene expression changes in addition to gene inactivation may eventually be required to assist therapeutic decision-making.

MODELLING DERIVATIONS AND CAVEATS

Models can be derived from either: 1) deductive reasoning—construction of a model from known scientific principles and using it to predict results in particular conditions, or 2) inductive reasoning—empirical observations of particular experimental or treatment conditions are used to construct a model which predicts the observed results.

Mathematical models are provisional, require appropriate caveats and frequently need further refinements for specific applications. All models should be reviewed when further knowledge or relevant data are available. Empirical models should only be applied within the same ranges as the original data used to obtain the model. A model which includes both deterministic and probability terms is likely to be a better approximation to reality in the biosciences because of the influence of random variation on biological parameter values.

WHY MODEL RADIOTHERAPY?

Radiation treatments usually follow standard (empirically derived) prescriptions, there being very little use of models in the prescription of radiotherapy. This is partly due to the failure of earlier formulations and partly because of the lack of accurate radiobiological data for individual patients. The development of models that can be used with data provided by predictive assays will inevitably lead to greater use of modelling techniques.

The lack of use of modelling in treatment prescription is in marked contrast to the long-standing use of sophisticated mathematics in treatment planning, dosimetry and imaging science. This paradox probably reflects the mistaken assumption that mathematics can be used to formulate the description of physical, but not biological, events.

Technical developments in radiotherapy can introduce not only physical changes but also differences in dose per fraction, dose rate, overall time, and so on. Following multiple simultaneous changes, it can be difficult to estimate which of these exert the greatest influence on clinical outcomes. Such situations ideally require the use of modelling to estimate the *separate* contributions of physical changes and biological parameter variations to treatment outcome. The alternative is to perform a complex series of randomized clinical trials: such exhaustive approaches could not only take many years to fulfil but also consume considerable resources. Mathematical modelling should potentially occupy a central role in the process of decision-making when multiple parameters contribute to the outcome of radiotherapy. Modelling can be used to:

(a) identify potentially dangerous treatment schedules,
(b) optimize treatment outcomes,
(c) design better clinical trials, and
(d) test medico-legal issues.

The interacting factors which can be utilized in modelling exercises are illustrated in Fig. 1. Practical examples of where modelling has been found useful include assessments of:

1. Over and under dosage in the gap or overlap regions between two adjacent treatment fields (5).
2. Changes in biological effect caused by variations inherent in treatment planning and treatment prescription (6).
3. The incremental increase in target dose per fraction due to air cavities in pituitary radiotherapy (7).
4. Changes in prescribed dose required to account for variation in normal tissue radiosensitivity (8).
5. Patients suitable for accelerated radiotherapy (9, 10).
6. Effect of changing brachytherapy source dwell times (11, 12).

RADIATION EFFECT MODELS

Power law models

The separation of the time and fractionation components and the dominant effect of the fractionation exponent in the power law found by Ellis (13) applied only to acute skin effects (erythema and desquamation) and not to late effects such as fibrosis. Yet this model formed the basis of other empirical methods for adjustment of the total dose for changes in overall time or fraction number.

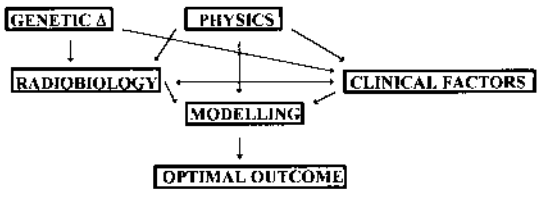

Fig. 1. Potential complex inter-relationships between radiation physics, genetic characterization (Δ), radiobiological parameters, clinical factors, mathematical modelling and optimal outcome.

$$D = NSD \cdot N^x \cdot T^y \quad [1]$$

Here, D is the total dose, NSD the nominal standard dose, N the number of fractions, T the overall treatment time. Data fitting gave respective values for x and y of 0.24 (for 5 fractions per week) and 0.11. This purely empirical model required substantial modification for applications to late reacting tissues (an increase in the fractionation and a reduction in time exponents, respectively) (14). This model is too rigid for complex biological tissues, cannot be extrapolated to all tissues, leads to errors at low numbers of fractions and overestimates the increase in total dose with treatment hyperfractionation (15, 16).

Linear Quadratic model

The Linear Quadratic (LQ) model of radiation effect is probably the best currently available model (17). It was originally an empirical model used to fit radiation chromosome damage (18) and growth suppression (19). The use of separate coefficients (α and β) for the separate types of lethal radiation damage relate well to both single fraction treatments and the process of fractionated radiotherapy (20, 21). The model is adaptable to different tissue types (early and late reacting) and satisfies the requirement that isoeffective dose will not increase continuously with fraction number.

The LQ model was deduced from first principles by separate consideration of: (i) DNA base pair damage by one high linear energy transfer (LET) ionization event or by two interacting lowLET ionizations (22); (ii) molecular events and their repair (23), or the rates of formation of non-repairable and potentially repairable DNA damage and repair processes (24).

The surviving fraction of cells (S) is expressed as

$$S = e^{-(\text{NUMBER OF LETHAL LESIONS})} \quad [2]$$

and in LQ form as

$$S = \exp[-\alpha d] \cdot \exp[-\beta d^2] \quad [3]$$

The (negative) logarithm of the surviving fraction is then related to radiation dose as

$$-\ln S = \alpha d + \beta d^2 \quad [4]$$

where d is the single dose.

The term $-\ln S$ can be replaced by E, defined as the radiation log cell kill so that

$$-\ln S = E = (\alpha d + \beta d^2) \quad [5]$$

For fractionated radiotherapy

$$E = n(\alpha d + \beta d^2) \quad [6]$$

where n is the number of fractions and the total dose $(D) = nd$.

Table 1

Calculated optic chiasm total doses (TD), rounded to the nearest 2 Gy, due to the air cavity effect and other errors inherent in treatment planning. The intended dose is 50 Gy in 25 fractions. Two values of α/β ratio relevant for neural tissue are tested. Modified from reference (9), Br J Radiol, with permission

Physical Dose Increment: (reduced beam attenuation + all planning errors) (%)	*TD* in 2 Gy Fractions ($\alpha/\beta = 1$ Gy)	*TD* in 2 Gy Fractions ($\alpha/\beta = 3$ Gy)
2.5	52	52
5.0	54	54
7.5	56	56
10.0	58	58

Biological Effective Dose (BED)

This useful concept allows easy comparison of different radiation schedules. The development of isoeffect calculations (25, 26) allowed the use of tissue-specific fractionation sensitivity, defined by α/β. The BED is found by dividing both sides of equation 6 by α

i.e.

$$\text{BED} = \frac{E}{\alpha} = D\left[1 + \frac{d}{\alpha/\beta}\right] \quad [7]$$

The bracketed term in equation [7] is the relative effectiveness (RE), so that BED = Total Dose × Relative Effectiveness.

The BED model represents the dose required for a given effect when delivered by infinitely small doses per fraction or at very low dose rates in the case of continuous radiation. Thus, to achieve isoeffectiveness between two fractionation schedules of total doses D_1 and D_2 and dose per fractions of d_1 and d_2 respectively:

$$D_1\left(1 + \frac{d_1}{\alpha/\beta}\right) = D_2\left(1 + \frac{d_2}{\alpha/\beta}\right) \quad [8]$$

and α/β ratios can be estimated if parameters D_1, D_2 and d_1 and d_2 are known.

Relatively fixed generic values of α/β derived from inbred animal experimental studies may not be representative of human populations because of natural variation in α and β values in the latter. Even for tumours of similar histology, radiosensitivity variations are a potentially significant factor affecting the reliability of the BED concept in the retrospective analysis of heterogeneous clinical data.

BED calculations can be used to express the equivalent total dose in 2 Gy fractions for a given isoeffect. Such a method provides clinicians with a familiar yardstick where a risk estimate is required, for example the equivalent total dose in 2 Gy fractions at the optic chiasm, where there is reduced beam attenuation due to air cavities (see Table 1). Such a method is relatively insensitive to changes in the tissue α/β ratio due to the approximation made to express the total dose in whole 2 Gy fractions in this example.

Fractionation sensitivities: (α/β) ratios

These may be derived from data sets where different fractionation schedules have been used to achieve a common clinical endpoint (27). Typical α/β values are 10–30 Gy for squamous cell carcinomas (28, 29) and 4 Gy for breast cancer (30). Brenner and Hall have recently estimated the prostate cancer value to be only 1.5 Gy (31). There is an urgent need to determine this important parameter in all human tumours. Normal tissue α/β ratios are generally smaller (1–4 Gy) than those for experimental cancers and many human tumours.

Repopulation

The inclusion in the LQ model of the effect of cells newly produced during treatment was an important advance (21), the modified cell kill at time t being:

$$E_t = n(\alpha d + \beta^2) - 0.693\frac{1}{T_{\text{eff}}} \quad [9]$$

where T_{eff} is the effective clonogen doubling time. For clinical situations where there is an apparent time delay before significant repopulation is detectable, a simple time delay factor (T_{k}) can be used:

$$E_t = n(\alpha d + \beta d^2) - 0.693\left(\frac{t - T_{\text{k}}}{T_{\text{eff}}}\right) \quad [10]$$

It must be emphasized that equation [10] is *only* applicable when $t > T_{\text{k}}$ (erroneous values of E will be obtained when these conditions are not fulfilled, for example in the case of highly accelerated schedules).

A more mechanistic approach is to include the potential doubling time T_{pot} and the cell-loss factor, the latter being likely to decrease during radiotherapy because of improved tumour microvascular perfusion. The cell-loss factor (ϕ or CLF) can be defined as the probability that newly created cells will die of causes such as hypoxia and insufficiency of nutrients and growth factors. Thus, $(1-\phi)$ represents the probability that new cells will survive. After integration, to allow for the likelihood that there is a slow exponential reduction in ϕ (at a rate constant v) due to improved perfusion during treatment (32), the net result is

$$E = n(\alpha d + \beta d^2) - \frac{\ln 2}{T_{\text{pot}}}\cdot\left(t - \frac{\phi_0}{v}(1 - \exp[-vt])\right) \quad [11]$$

where ϕ_0 is the pretreatment CLF. This result may be used to simulate the time course of tumour cell accelerated repopulation data sets, as shown in Fig. 2.

Repair

When using multiple fractions per day there may be a reduction in CNS tissue tolerance owing to incomplete repair between fractions. Simple exponential repair models (derived empirically) have not fully explained these effects and many authors have postulated biexponential repair (fast and slow) mechanisms. Fowler currently advocates a more fundamental approach, based on a physical-chemistry approach and where repair rate is a second-order process. This repair model predicts more unrepaired damage at longer intervals of time (e.g. 12–24 h) than in the case of the conventional monoexponential first-order models. The subsequent incomplete repair equations derived by Dale et al. allow for a considerably safer calculation of isoeffective doses for multiple radiotherapy fractions per day.

Hypoxia

Lack of oxygen reduces cell kill. For modelling purposes the simplest assumption is that oxygen is purely dose modifying (33). The reduced cell kill which occurs in hypoxic tumours is given as (34):

$$E = n\left(\frac{\alpha d}{q_\alpha} + \frac{\beta d^2}{q_\beta^2}\right) \quad [12]$$

where q_α and q_β are respectively the limiting values of oxygen enhancement ratios (OERs) at small and large doses per fraction. Equations that allow for the OER to change with a wide range of fraction size, are available (35). Two compartment models (hypoxic and oxic), where a flux of cells between the two compartments represents the process of reoxygenation, and where repopulation occurs in the oxic compartment, have been described and merit greater attention (36, 37).

Tumour cure probabilities, clonogen numbers and heterogeneity/population effects

Tumour cure probability (TCP) can be estimated by use of Poisson statistics (38). For a tumour initially comprising C_0 clonogenic cells, TCP is expressed as a function of the number of surviving clonogenic cells, C_t at time t, when E_t is the log cell kill given in equation 6.

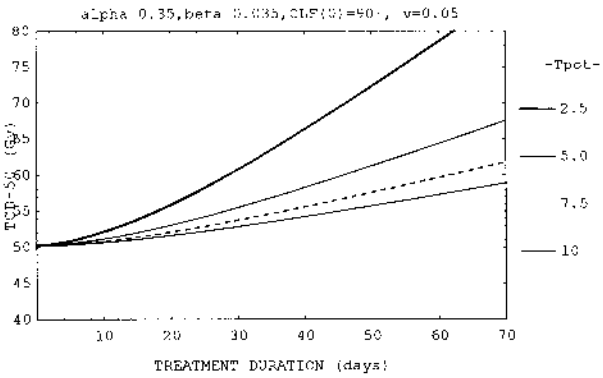

Fig. 2. Modelled generic curves for accelerated repopulation. The 50% tumour cure dose is plotted against treatment duration for variable values of T_{pot} which governs the final slope. The rate of change in the cell loss factor is assumed to be at 5% per day from a pre-treatment ϕ value of 90%. For further modelling examples, see reference (32).

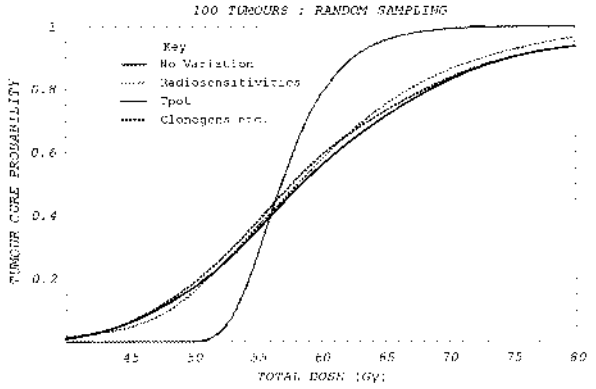

Fig. 3. Relationship between tumour cure probability (TCP) and total dose (*TD*) in four settings: 1) no variation in parameters in the LQ model (equation 9), and then sequential inclusion of random variation in the parameters given in equation 11 for 2) radiosensitivities, 3) potential doubling times, and 4) clonogen numbers, cell loss factors and rates of change in cell loss factor.

$$C_t = C_0 \cdot e^{(-E_t)} \quad [13]$$

$$TCP = e^{(-C_t)} \quad [14]$$

Equation 14 is obtained from the Poisson distribution, where the probability of complete success (TCP = 1) is the special case of there being no surviving cells after therapy.

Dose–response curves constructed from this relatively simple model describe the response of individual tumours and have particularly steep slopes. Dose–response curves for a population of tumours are considerably less steep, probably due to inter-tumour heterogeneity of the parameters which determine tumour cure (39).

A less steep curve can be achieved from the Poisson model by use of multiple calculations utilizing variable radiobiological and physical parameters to simulate inter-tumour and treatment-related heterogeneity (40–42). Fig. 3 shows how the dose–response curves generated for equation 9 become progressively less steep with the introduction of randomly selected variations in the radiobiological parameters. These variations allow for greater curability at lower doses and greater incurability at higher doses, the net effect being to flatten the curve. The slope at the 37% cure probability level (where there is an expected one surviving clonogenic cell, since $e^{-1} = 0.37$) is reduced by a factor of approximately 3 in this example. The statistical ranges assumed for these random sampling calculations are presented in Table 2. It should be noted that in this case there is very little further change in the dose–response slope after the radiosensitivity parameter variations are included. However, the use of a much wider range of clonogen numbers would further reduce the dose–response slope. Thus, with some modification, the Poisson method can be used to study the estimated cure probabilities for whole populations of tumours or specific subgroups.

The alternative to Poisson statistics is the Logistic model (43), which produces the less steep dose–response curves characteristic of tumour populations. This method requires only one (average) value for each radiobiological parameter, but the outcome for population subgroups cannot then be considered. The logistic model is consequently less comprehensive (41) and cannot be used to optimize individual treatment schedules.

A further option is to use predefined tumour dose–response slopes or gamma factors (44). These factors normally refer to 2 Gy per fraction schedules. For alternative fractionation schedules, use of gamma factors defined as the percentage change in effect per 1% change in BED is required. There are difficulties when applying gamma factors derived from population data to individual patient risk estimation, because of the steeper slope in the latter case.

Similar models exist for the calculation of normal tissue complication rates. These may include volume-related effects based upon empirical modelling and limited clinical dose–response data (45). Ideally, allowance should be made for hierarchical organization of tissues, delayed repopulation, consequential radiation damage, age, vascular status, concomitant medical conditions and previous trauma or surgery, since all these factors can influence radiation tolerance (46–49). The existing (rather physical) NTCP models are complex to handle and have little biological basis: the use of simpler BED isoeffect calculations is reasonable until better predictive models are found.

A further uncertainty inherent in the calculation of TCP is the number of pretreatment clonogens. These are often derived inductively from existing clinical data sets where a given dose schedule will result in a known TCP. Clonogen numbers of 10^7–10^9 are usually used, based on the assumption that 1 g tumour tissue will normally contain approximately 10^9 cells. In larger human tumours, if only 1–10% of cells are clonogenic, a 100 g tumour could contain 10^8–10^9 clonogens.

Table 2

Details of statistical distributions used for random sampling calculations. The normal distribution is assumed, with the exception of the T_{pot} where a log–normal distribution is used

Parameter	Mean value	Standard deviation
α (radiosensitivity)	0.35 Gy^{-1}	0.05 Gy^{-1}
β (radiosensitivity)	0.035 Gy^{-2}	0.005 Gy^{-2}
ϕ_0 (pre-treatment cell loss factor)	0.88	0.02
v (rate of change of ϕ)	0.06 day^{-1}	0.01 day^{-1}
T_{pot} (potential doubling time)	5 days (log)	1.5 days (log)
C (clonogen number)	5×10^8	2×10^8

Variations in clonogen numbers can be used to simulate the treatment of tumours of different volumes and hence the impact of earlier cancer detection or the influence of surgical debulking on cell kill or TCP following radiotherapy (41, 50). Similar considerations apply to normal tissues where tissue rescuing units or other functional units (45, 46, 51) are used.

Derivation of radiobiological parameters from clinical data sets

By application of the above equations already delineated to the head and neck cancer data compiled by Withers et al. (28), the following radiobiological parameters may be indirectly estimated:

1. Clonogen doubling times seem to be around 40 days during the first month of treatment and then shorten to approximately 4 days (28).
2. Providing that improved microvascular perfusion promotes accelerated repopulation, the pretreatment cell loss factor (ϕ_0) is the ratio of the initial and final slopes of the TCD_{50} versus treatment duration plot (32). The estimated (ϕ_0) value is approximately 90%, which is compatible with known values.
3. The half-life of the effective reoxygenation rate over 25–30 days is approximately 5–6 days. It follows that the rate constant is approximately 0.693/6, i.e. $\sim 10\%$ day^{-1} (52).
4. The initial hypoxic fraction is estimated as 10–50% depending upon which value of OER (and therefore oxygen tension) is assumed (52).

Loss of tumour control with time

The loss of tumour control rate with time can be expressed as $-d(TCP)/dt$ and is therefore dependent on the expected TCP value at any instant (41). The form of this relationship is seen in Fig. 4, where the maximum rate of change in TCP occurs at a TCP value of 37%. Loss of local control is 1–2% per day of treatment extension in population studies and in heterogeneous population modelling using random sampling. The effect appears greatest in stage III cancers, where the expected tumour control rate is around 30–50%. Smaller tumours (stage I), for which a higher TCP is expected, may only show the same rate of control loss at much longer overall times. Modelling techniques have been applied to the frequently occurring problem of how to compensate for unscheduled treatment interruption (53–55).

Optimization of radiotherapy fractionation by modelling

Overall time can be optimized (56, 57). To optimize dose per fraction in order to maximize tumour cell kill while maintaining a normal tissue isoeffect, the following method has been used (58, 59). Cell kill is expressed in terms of tumour dose per fraction (z), normal tissue dose per fraction (d), the average inter-fraction interval (f), the normal tissue α/β ratio (k), the normal tissue geometrical sparing factor (g) so that $z = gd$, and the average clonogen doubling time (T_{eff}). By equating the first differential coefficient (dE/dz) with zero, the resulting optimum dose per fraction is given by the solution for z in:

$$(\beta k T_{eff} - \alpha g T_{eff})z^2 + 1.386fgz + 0.693fk = 0 \quad [15]$$

The optimum dose per fraction *increases* with shortening of the doubling time, and respective reduction of radiosensitivities, the g factor, and when the tumour α/β ratio is reduced in order to be close to the normal tissue value. For the majority of situations encountered in conventional radiotherapy given when the interfraction interval (f) is approximately 1.4 days, which represents 5 fractions per 7 days (days) (7 days/5 fractions = 1.4 days), the optimum dose per fraction is 1.7–2.5 Gy when the g factor is 1.0, which corresponds well with clinical experience (see Fig. 5a).

Fig. 5b includes calculations for a heterogeneous population of 200 tumours with randomly selected parameter variations similar to the previous examples. In this example, the geometric sparing factor (g) is 0.75 (as may occur in focal forms of radiotherapy) and consequently the optimum dose per fraction increases and is approximately 4 Gy per fraction for $f = 1.4$ days (i.e. 5 fractions per week). The introduction of parameter variations produces considerably less variation in cell kill with dose per fraction, but the optimum dose per fraction turnover points remains and such predictions are theoretically testable in the laboratory and clinic. Studies of this kind, which are essentially mathematical preclinical trials, could be used to guide clinicians in the choice of appropriate dose fractionation schedules in fractionation trials.

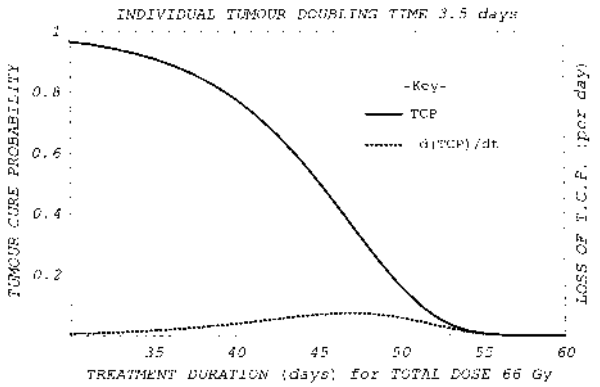

Fig. 4. Relationship between TCP and treatment duration with no variation in parameters in equation 9. Also shown is the differential coefficient ($-d(TCP)/dt$), the rate of loss in TCP with time (expressed here as a fraction of unity per day). The maximum loss of tumour control with time in this tumour ($\alpha = 0.35$ Gy^{-1}, $\beta = 0.035$ Gy^{-2} $T_{eff} = 3$ days, 5×10^8 clonogens) rises to approximately 7% per day at around 39 days when the TCP falls to 37%. Further modelling in references (41, 54, 56).

Cost modelling

Modelling of overall costs based upon the cost per fraction and the cost of treatment failure, based on a failure-related cost $\times (1 - \text{TCP})$, can be used to investigate the potential cost implications of various aspects of radiotherapy (50, 59). The optimal dose per fraction derived from the cost model is not identical to the biologically optimized dose per fraction discussed above. In general, the extra initial costs of more complex fractionation schedules and/or greater treatment sophistication are seen to be justified when good gains in TCP and reduced overall cost are predicted.

Selection of treatment technique

Use of an optimization method, as outlined above, does emphasize the instances where treatments may need to be specially adapted; for example:

1. accelerated hyperfractionated radiotherapy, for tumours with short tumour clonogen doubling times,
2. more focal forms of radiotherapy, in order safely to provide a higher total dose to more radioresistant tumours, or
3. for tumours with rapid clonogen repopulation and intrinsic radioresistance, by a combination of both the above approaches.

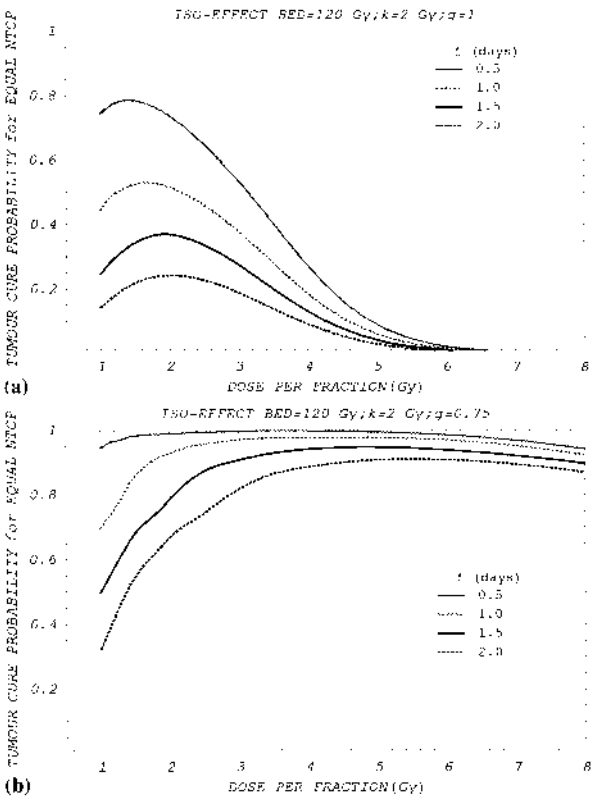

Fig. 5. TCP for equal late tissue effect of 120 Gy BED plotted against tumour dose per fraction for variable inter-fraction intervals (f) and where there is (a) no normal tissue sparing and (b) where there is normal tissue sparing ($g = 0.75$) for 200 tumours using random sampling in all radiobiological variables with accelerated repopulation. Further examples can be found in references (58, 59).

The separate contributions of radiosensitivity and doubling times to the cure probabilities require to be known before a rational decision can be made. One way of achieving this is to calculate the partial differential coefficient for each parameter e.g. $\mathrm{d(TCP)/d}\alpha$ and $\mathrm{d(TCP)/d}(T_{\mathrm{eff}})$. The ratio of these two derivatives provides the relative importance of these two parameters. This approach may also be of help in making a decision about which form of molecular/gene biotherapies (which may specifically target radioresistance or proliferation) to use during radiotherapy in individual patients (vide infra). For example, where $\mathrm{d(TCP)/d}\alpha$ far exceeds $\mathrm{d(TCP)/d}T_{\mathrm{eff}}$, then the use of therapies which change radiosensitivity (and/or the use of a higher dose by focal radiotherapy) will have a greater impact on TCP than biotherapies designed to reduce repopulation (and/or the use of accelerated radiotherapy).

Tumour volume changes and brachytherapy

Modelling of brachytherapy has been extensively reviewed (60). The inevitable physical dose gradients and temporal variations in treatment application do interact with the classical radiobiological parameters. Conversion of physical to biological dose is possible through special adaptations of the LQ model. The optimal timing of brachytherapy relative to external beam radiotherapy (teletherapy) will depend on the tumour repopulation and shrinkage rates. Teletherapy is frequently given to large treatment volumes, including the primary tumour and surrounding areas of potential microscopic tumour infiltration and nodal metastases. Any tumour shrinkage will allow for an increase in tumour dose at subsequent brachytherapy, providing this is prescribed at a standard distance. The brachytherapy kill will vary with time, as is shown in the example in Fig. 6. The tumour cell kill will improve with time only if the tumour repopulation rate is insufficient to overcome the dose advantage gained due to continuing tumour regression. Adverse combinations occur when the tumour cell doubling time is short and the regression rate is slow: in such cases either 1) brachytherapy should be used sooner (during or before teletherapy), or 2). additional treatment modalities such as chemotherapy are indicated after teletherapy in order to minimize repopulation, while allowing tumour shrinkage to continue to a stage where brachytherapy can be effectively used.

The geometric conditions of treatment can also exert a marked influence. For example, in the placement of linear brachytherapy sources in intralumenal therapy, poor source positioning relative to the tumour centre can negate the potentially beneficial effect of shrinkage. Similarly, the inter-fraction interval for fractionated high-dose rate

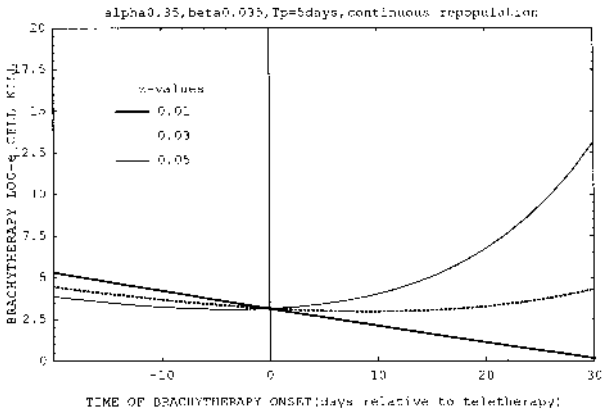

Fig. 6. Modelled relationship between brachytherapy cell kill and time relative to teletherapy, which is assumed to cease at $t = 0$. The tumour linear shrinkage rate (z per day) is varied and the effective doubling time is assumed to be 5 days. Further modelling references are given in reference (60).

(HDR) brachytherapy is shown to be related to the ratio of the regression rate and the tumour effective doubling time, so that in the majority of clinical situations modelling studies predict that the inter-fraction interval should be kept reasonably short.

The occurrence of steady-state exponential tumour volume regression commences during the first week of teletherapy in cervix cancer (63). If accelerated repopulation effectively commences at around 21–28 days during teletherapy of squamous cancers, then brachytherapy should ideally be performed at around this time, when the dose benefits of tumour shrinkage will not be opposed by significant repopulation. Table 3 shows the use of computer random sampling methods in the attempted optimization of the time of onset of HDR brachytherapy relative to teletherapy (45).

The use of gene-specific therapies offers a future prospect for prevention of accelerated repopulation, which could then provide greater scope for using brachytherapy (or other focal forms of radiotherapy) to small residual tumour volumes at longer time intervals after teletherapy (60).

Genetic and molecular biology interactions with radiotherapy

It is timely to assess the potential impact of new molecular-based biotherapies designed from tumour genetic research by modelling studies. Radiosensitization by various methods have been simulated by Wheldon et al. (61). The fact that antisense therapy exposures of up to 14 days can induce useful tumour kill (62) should be of considerable significance in radiotherapy, where changes in cellular phenotype for periods of even 7–14 days could exert significant benefits. Fig. 7 illustrates the estimation of improved TCP where 1) repopulation is halted for a variable duration (*x days*) by the biotherapy, and 2) the cell population is radio-sensitized for a variable number of treatment fractions.

Even in heterogeneous populations, involving widely varying biological parameters, substantial gains in tumour control are predicted. Equations for these scenarios are presented in the Appendix. The authors have also developed a more complex model, allowing for variations in blood flow and, consequently, the delivery of biotherapies to a variable proportion of cells during radiotherapy.

Mechanisms and hypotheses

Modelling can help create testable scientific hypotheses. Recent MR imaging studies of patients with cervical cancer showed that the tumour shrinkage rate correlated well with the percentage change in gadolinium concentration during the first 2 weeks of radiotherapy ($p < 0.05$) (J. Brunt, pers. comm.). Tumours with increased gadolinium uptake at 2 weeks shrink rapidly, and vice versa. Gadolinium uptake depends on blood flow and vascular permeability. Tumour regression rate may therefore be determined by the prevailing tumour blood flow that will control the efficiency of the rate-limiting process of dead

Table 3

TCP values for four teletherapy (45 Gy in 25 fractions given over 35 days) and high dose rate brachytherapy (HDRB) schedules (3 × 6 Gy at 1 cm from a line source inserted through the centre of a spherical tumour measuring 3 cm at the onset of all therapy)

	TCP (random 1)	TCP (random 2)	TCP (random 3)
Schedule A $S = 0$ days, $T = 35$ days	0.209	0.258	0.318
Schedule B $S = 14$ days, $T = 42$ days	0.232	0.294	0.343
Schedule C $S = 28$days, $T = 56$ days	0.202	0.282	0.315
Schedule D $S = 36$ days, $T = 40$ days	0.330	0.390	0.453

Schedule A: HDRB commences on day 1 and is repeated at 14-day intervals (overall time $T = 35$ days, with final brachytherapy treatment at 28 days).
Schedule B: HDRB commences on day 14 and is repeated at 14-day intervals ($T = 42$ days).
Schedule C: HDRB commences on day 28 and is repeated at 14-day intervals ($T = 56$ days).
Schedule D: HDRB commences on day 36 and is repeated at 2-day intervals ($T = 40$ days).
Calculations assume a population of 100 tumours with random selection of tumour shrinkage rates, α, β, C, v, T_{pot} and ϕ_0. The symbol S refers to the time interval between the onset of teletherapy and the first fraction of brachytherapy. Three randomization exercises are given.

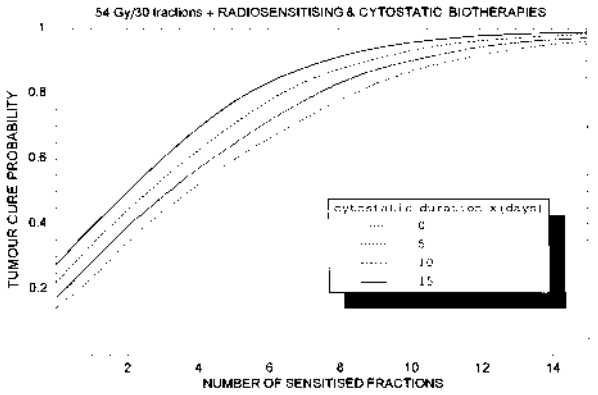

Fig. 7. Tumour cure probabilities plotted against the number of biotherapy-sensitized fractions (by a factor $s = 1.5$) for 200 tumours treated to a total of 30 fractions at 1.8 Gy per fraction. Cytostatic biotherapy is also used for a variable duration (x days) in tumours where there is continuous repopulation (mean $T_{eff} = 5$ days). The parameter variations are given in Table 2. References (37, 38, 71) consider radiosensitization modelling.

cell clearance, particularly since tumours do not possess a lymphatic system that performs this function in normal tissues. The observed gadolinium changes show that tumours may either undergo reduced or enhanced microcirculation flow rates as a response to radiotherapy. In the former case, a chaotic tumour vascular structure such as that found in poorly differentiated tumours could further deteriorate because of enhanced killing of vascular cells relative to tumour, causing more A–V shunting, etc., so that the cell loss factor would initially increase and the hypoxic fraction would remain relatively high. The net result is that, regardless of the T_{pot} value, there is little or no effective repopulation during radiotherapy.

Where blood flow rates can progressively improve, owing to a more ordered vascular structure as found in more well-differentiated tumours, the cell loss factor decreases. As a result, the hypoxic fraction falls to a low value (after the inevitable initial increase due to selective killing of oxic cells) and there is very effective repopulation during the latter half of radiotherapy. Thus even if both these tumour types had a T_{pot} value of 5 days, accelerated repopulation during therapy will only occur in the 'rapidly shrinking' tumour. These hypothetical examples are modelled in Fig. 8 and the equations presented in the Appendix. These models are testable by sequential dynamic CT, MR and PET imaging studies (63–66) and also by oxygen microelectrode studies (67). There is some evidence that accelerated repopulation is restricted to the more well-differentiated squamous carcinomas (68). This hypothesis can explain why pretreatment T_{pot} alone is not a very good indicator for outcomes after accelerated radiotherapy (69).

CONCLUSION

A greater appreciation of the scope, applications and limitations of radiobiological modelling is required within radiation oncology. There will probably be increasing applications of modelling in practical situations such as treatment planning dose volume analysis (70), optimization of therapy determined by predictive assays, schedule design in clinical trials, testing applications of new biotherapies, in hypothesis development and medico-legal cases (71).

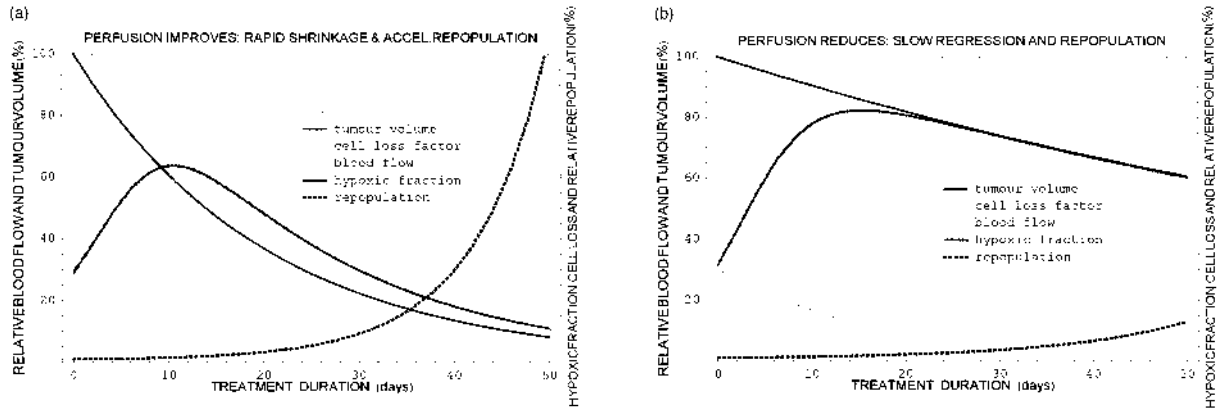

Fig. 8. Hypothetical model of two tumours—*each with a T_{pot} of 5 days*, (a) in which a relatively well-ordered pretreatment tumour circulation allows for a progressive improvement in tumour perfusion during radiotherapy. The cell loss factor, hypoxic fraction (after an initial increase) and tumour volume reduce relatively rapidly (c. 5% per day). There is effective repopulation during radiotherapy, particularly after 20–30 days has elapsed. (b) In which a *chaotic* pretreatment tumour circulation produces an initial reduction in absolute tumour perfusion, followed by a very slow reduction in the hypoxic fraction, and therefore a slow reduction in cell loss factor and shrinkage rate. There is very little repopulation during radiotherapy, regardless of the pretreatment T_{pot} value.

ACKNOWLEDGEMENTS

Dr OCA Scott, Professors H. M. Warenius, J. F. Fowler and J. Denekamp are thanked for their encouragement over many years. We also thank the Clatterbridge Cancer Research Trust and Endowment Funds for financial support.

REFERENCES

1. Malthus TR. An essay on the principles of population. In: Hoppensteadt FC, ed. Mathematical methods of population biology. Cambridge(reprinted 1982): Cambridge University, 1798.
2. D'Arcy Thompson. On growth and form. Cambridge(reprinted 1994): Cambridge University, 1917.
3. Maynard Smith J. Mathematical ideas in biology. Cambridge: Cambridge University, 1971.
4. Hall EJ. Radiobiology for the radiologist. Philadelphia: JB Lippincott, 1994.
5. Cederbaum M, Kuten A. The time-dependent LQ model applied to the matching line of adjacent fields in radiotherapy. Radiother Oncol 1994; 31: 181–3.
6. Scalliet P, Cosset J-M, Wambersie A. Application of the LQ model to the interpretation of absorbed dose distribution in the daily practice of radiotherapy. Radiother Oncol 1991; 22: 180–9.
7. Jones B, Samarasekara S, Tan LT, Mayles WPM. The influence of air cavities on the optic chiasm dose during pituitary radiotherapy for acromegaly. Br J Radiol 1996; 69: 723–5.
8. Tucker SL, Geara FB, Peters LJ, Brock WA. How much could the radiotherapy dose be altered for individual patients based on a predictive assay of normal tissue radiosensitivity? Radiother Oncol 1996; 38: 103–14.
9. Tucker SL, Chan K. The selection of patients for accelerated radiotherapy on the basis of tumour growth kinetics and intrinsic radiosensitivity. Radiother Oncol 1990; 18: 197–211.
10. Fowler JF. How worthwhile are short schedules in radiotherapy? A series of exploratory calculations. Radiother Oncol 1990; 19: 165–81.
11. Jones B, Tan LT, Freestone G, Bleasdale C, Myint S, Littler J. Non-uniform dwell times in line source high dose rate brachytherapy: physical and radiobiological considerations. Br J Radiol 1994; 67: 1231–7.
12. Scalliet P, Vanneste F, Octave-Prignot M. Do stepping sources differ from linear sources regarding their biological effectiveness? Radiother Oncol 1997; (Suppl 1) 43: S7.
13. Ellis F. Dose time and fractionation; a clinical hypothesis. Clin Radiol 1969; 20: 1–7.
14. Sheline GE, Wara WM, Smith V. Therapeutic irradiation and brain injury. Int J Radiat Oncol Biol Phys 1980; 6: 1215–28.
15. Bates TD, Peters LJ. Danger of the clinical use of the NSD formula for small fraction numbers. Br J Radiol 1975; 48: 773.
16. Liversage WE. A critical look at the ret. Br J Radiol 1971; 44: 91–100.
17. Joiner MC. The linear-quadratic approach to fractionation. In: Steel GG, ed. Basic clinical radiobiology. London: Edward Arnold, 1993: 55–64.
18. Lea DE, Catcheside DG. The mechanism of induction by radiation of chromosome aberrations in Transcendentia. J Genet. 1942; 44: 216–45.
19. Gray LH, Scholes ME. The effect of ionising radiations on the broad bean root. Br J Radiol 1951; 24: 285–91.
20. Thames HD, Hendry JH. Fractionation in radiotherapy. London: Taylor and Francis, 1987: 148–63.
21. Fowler JF. The linear quadratic formula and progress in fractionated radiotherapy. Br J Radiol 1989; 62: 679–94.
22. Kellerer AM, Rossi HH. The theory of dual radiation action. Radiat Res 1978; 75: 471–88.
23. Chadwick KH, Leenhouts HP. The molecular theory of radiation biology. Berlin: Springer, 1981.
24. Curtis SB. Lethal and potentially lethal lesions induced by radiation—a unified repair model. Radiat Res 1986; 106: 252–70.
25. Barendsen GW. Dose fractionation, dose rate and iso-effect relationships for normal tissue responses. Int J Radiat Oncol Biol Phys 1982; 8: 1981–97.
26. Dale RG. The application of the linear quadratic theory to fractionated and protracted radiotherapy. Br J Radiol 1985; 58: 515–28.
27. Withers HR, Thames HD, Peters LJ. A new isoeffect curve for change in dose per fraction. Radiother Oncol 1983; 1: 187–91.
28. Withers HR, Peters LJ, Taylor JMG, et al. Local control of carcinoma of the tonsil by radiation therapy: an analysis of patterns of care in nine institutions. Int J Radiat Oncol Biol Phys 1995; 33: 549–62.
29. Withers HR, Taylor JMG, Maciejewski B. The hazard of accelerated tumour clonogen repopulation during radiotherapy. Acta Oncol 1988; 27: 131–46.
30. Douglas BG. Implications of the quadratic survival curve and human skin radiation 'tolerance doses' on fractionation and super-fractionation dose selection. Int J Radiat Oncol Biol Phys 1982; 8: 1135–42.
31. Brenner D, Hall E. (personal communication).
32. Jones B, Dale RG. Cell loss factors and the linear quadratic model. Radiother Oncol 1995; 37: 136–9.
33. Alper T. Cellular radiobiology. Cambridge: Cambridge University, 1979.
34. Wouters BG, Brown JM. Cells at intermediate oxygen levels can be more important than the 'hyopoxic fraction' in determining tumour response to fractionated radiotherapy. Radiat Res 1997; 147: 541–50.
35. Dasu A, Denekamp J. New insights into factors influencing the clinically relevant oxygen enhancement ratio. Radiother Oncol 1998; 46: 269–77.
36. Denekamp J, McNally NJ, Fowler JF, Joiner MC. Misonidazole in fractionated radiotherapy: are many small fractions best? Br J Radiol 1980; 53: 981–90.
37. Scott OCA. Mathematical model of repopulation and reoxygenation in radiotherapy. Br J Radiol 1990; 63: 821–3.
38. Porter EH. The statistics of dose/cure relationships for irradiated tumours. Br J Radiol 1980; 53: 210–27.
39. Tucker SL, Thames HD, Taylor JMG. How well is the probability of tumour cure after fractionated irradiation described by Poisson statistics? Radiat Res 1990; 124: 273–82.
40. Withers HR. Biological basis of radiation therapy. In: Perez CA, Brady LW, eds. Practice of radiation oncology. Philadelphia: JP Lippincott, 1992: 64–96.
41. Jones B, Dale RG. The reduction in tumor control with increasing over all time mathematical considerations. Br J Radiol 1996; 69: 830–8.
42. Jones B. The developement of mathematical models in rediation oncology. MD thesis, University of Cambridge, 1997.
43. Thames HD, Rozell ME, Tucker SL, Ang KK, Fisher DR, Travis E. Direct analysis of quantal response data. Int J Radiat Oncol Biol Phys 1986; 49: 999–1009.
44. Brahme A. Dosimetric precision requirements in radiation therapy. Acta Radiol Oncol 1984; 23: 379–91.

45. Niemierko A, Goitein M. Calculation of normal tissue complication probability and dose-volume histogram reduction schemes for tissues with a critical element architecture. Radiother Oncol 1991; 20: 166–76.
46. Van Der Kogel AJ. Radiobiology of normal tissues. In: Steel GG, ed. Basic clinical radiobiology. London: Edward Arnold, 1993.
47. Hopewell JW, Wright EA. The nature of latent cerebral irradiation damage and its modification by hypertension. Br J Radiol 1970; 43: 161–7.
48. Hopewell JW. Mechanisms of action of radiation on skin and underlying tissues. Br J Radiol 1986; 19 (Suppl): 39–51.
49. Hopewell JW, Morris AD, Dixon-Brown A. The influence of field size on the late tolerance of the rat spinal cord to single doses of x-rays. Br J Radiol 1987; 60: 1099–108.
50. Dale RG, Jones B. Radiobiologically based assessments of the net costs of fractionated radiotherapy. Int J Radiat Oncol Biol Phys 1996; 36: 739–46.
51. Hendry JH, Thames HD. The tissue rescuing unit. Br J Radiol 1986; 59: 628–30.
52. Jones B, Dale RG. Estimation of tumour hypoxic fraction from clinical data sets compatible with accelerated repopulation. Acta Oncol 1998; 37: 263–8.
53. Wheldon TE, Barrett A. Radiobiological rationale for gaps in radiotherapy regimes by post-gap acceleration of fractionation. Br J Radiol 1990; 63: 114–9.
54. Dale RG, Sinclair JA. A proposed figure of merit for the assessment of unscheduled treatment interruptions. Br J Radiol 1994; 67: 1001–7.
55. Hendry JH, Bentzen SM, Dale RG, et al. A modelled comparison of the effects of using different ways to compensate for missed treatment days in radiotherapy. Clin Oncol 1996; 8: 297–307.
56. Fowler JF, Denekamp J, Sheldon PW, et al. Optimum fractionation in x-ray treatment of C3H mouse mammary tumours. Br J Radiol 1974; 47: 781–9.
57. Dale RG. Time-dependent tumour repopulation factors in the linear quadratic equations—implications for treatment strategies. Radiother Oncol 1989; 15: 371–82.
58. Jones B, Tan LT, Dale RG. Derivation of the optimum dose per fraction from the linear quadratic model. Br J Radiol 1995; 68: 894–902.
59. Jones B, Dale RG. Radiobiologically based assesments of the net costs of fractional focal radiotherapy. Br J Radiol 1998 (further details please)
60. Dale RG, Jones B. The radiobiology of Brachtherapy. Br J Radiol 1998; 71: 465–83.
61. Wheldon TE, Mairs RJ, Rampling RP, Barrett A. Modelling the enhancement of fractionated radiotherapy by gene transfer to sensitize tumor cells to radiation. Radiother Oncol 1998; 48: 5–13.
62. Webb A, Cunningham D, Cotter F, et al. BCL-2 antisense therapy in patients with non-Hodgkin's lymphoma. The Lancet 1997; 349: 1137–41.
63. Blomley MJK, Dawson P. Bolus dynamics: theoretical and experimental aspects. Br J Radiol 1997; 70: 351–9.
64. Leach MO. Quantitative assessment of tumour response using MRI/MRS. In: Faulkner K, et al., eds. Quantitative imaging in oncology. Proc 19th LH Gray Conference, Br J Radiol, 1996.
65. Mayr NA, Yuh WTC, Magnotta VA, et al. Tumour perfusion studies using fast magnetic resonance imaging technique in advanced cervical cancer: a new noninvasive predictive assay. Int J Radiat Oncol Biol Phys 1996; 36: 623–33.
66. Chapman JD, Engelhardt EL, Stobbe CC, et al. Measuring hypoxia and predicting tumour radioresistance in nuclear medicine assays. Radiother Oncol 1998; 46: 229–37.
67. Vaupel P, Hockel M. Oxygenation of human tumours, in blood perfusion and microenvironment of human tumours: implications for clinical radiotherapy. Berlin: Springer-Verlag, 1998: 63–72.
68. Hansen O, Overgaard J, Hansen HS, et al. Importance of overall treatment time for the outcome of radiotherapy of advanced head and neck carcinoma: dependency on tumour differentiation. Radiother Oncol 1997; 43: 47–52.
69. Begg AC. The clinical status of T_{pot} as a predictor? Or why no tempest in the T_{pot}!. Int J Rad Oncol Biol Phys 1995; 32: 1539–41.
70. Wheldon TE, Deehan C, Wheldon EG, Barrett A. The linear quadratic transformation of dose-volume histograms in fractionated radiotherapy. Radiother Oncol 1998; 46: 285–96.
71. Dische S, Joslin CAF, Millar S, Bell NL, Holmes JC. The breast injury litigation and the clinical oncologist. Clin Oncol 1998; 10: 367–71.

APPENDIX A

Molecular biotherapies

$$\mathrm{TCP} = \exp\left[-c \cdot \exp\left[-E_1 - E_2 + \frac{0.693}{T_{\mathrm{eff}}}(T-x) \right] \right] \quad [A1]$$

where E_1, and E_2, are the log cell kill values, i.e. $n(\alpha d + \beta d^2)$, in each respective phase, E_1 being the unsensitized conventional radiotherapy and E_2 that during the radio-sensitising biological therapy. If there are m fractions each sensitized by an average dose modifying factor s, then $E_2 = m(\alpha s d + \beta s^2 d^2)$. When the use of cytostatic biotherapy is effective for a duration x days, x is subtracted from T, the overall time.

Relationship between regression rate, ϕ, hypoxic fraction and repopulation

These graphics are constructed using equations given in the text but also assume that the same rate parameter (v) is approximately valid for the rate of change of ϕ, for the reoxygenation rate and regression rate constant.

Hypoxic fraction after n fractions approximates to

$$\frac{SF_{\mathrm{hyp}}^n}{SF_{\mathrm{hyp}}^n + SF_{\mathrm{ox}}^n} \cdot \exp[-vt] \quad [A2]$$

where SF_{hyp} and SF_{ox} refers to surviving fraction after 2 Gy in hypoxic and oxic conditions, respectively. The cell loss factor is assumed to follow the same time course as the hypoxic fraction when tumour blood flow is reduced during radiotherapy; where tumour blood flow increases during radiotherapy the ϕ is assumed to fall exponentially.

Regression rate is given by v in $V_t = V_0 \cdot \exp[-vt]$ where V refers to the tumour volume at times t and zero respectively.

The instance of a reduction in tumour blood flow (F) may be simulated by a general polynomial function, i.e.

$$F = -at + bt^2 - ct^3 \quad [A3]$$

For an increase in perfusion with time, a general asymptotic function is used:

$$yt = y_{\min} + (1 - \exp[-kt])(y_{\max} - y_{\min}) \quad [A4]$$

where $y_{\min}$ is the initial perfusion rate and $y_{\max}$ the final value, k being the rate constant.